Solar Neutrinos

W.C. Haxton
Institute for Nuclear Theory, Box 351550 and
Department of Physics, Box 351560
University of Washington, Seattle, WA 98195-1550, USA

K. Lande
Dept. of Astronomy/Astrophysics, University of Pennsylvania
Philadelphia, PA 19104-6396

S.P. Rosen
Dept. of Physics, University of Texas, Arlington
P.O. Box 19050, Arlington, TX 76019

We summarize the current status of the solar neutrino problem, emphasizing the difficulty of reconciling the results of the chlorine, Kamiokande, and SAGE/GALLEX experiments with plausible variations in the standard solar model. Several new experiments under construction or development will provide important new information on the flux, energy distribution, and flavor of solar neutrinos. We discuss the crucial role these experiments will play in testing the properties of the neutrino, including masses in the range predicted by many extensions of the standard electroweak model.

§1 Introduction

The prospect of quantitatively testing the theory of main-sequence stellar evolution provided much of the original motivation for measuring solar neutrinos: solar neutrinos carry, in their energy distribution and flux, a precise record of the thermonuclear reactions occurring in the sun's core. The predictions of the standard solar model (SSM) are more tightly constrained today than when the Homestake ^{37}Cl experiment was first mounted (almost three decades ago). Careful laboratory measurements and improved theory have helped to reduce uncertainties in the atomic and nuclear microphysics of the SSM, e.g., in nuclear reaction rates, radiative opacities, and the equation of state. The development of helioseismology has provided a new tool for probing the solar interior. Finally, we better understand our sun in the context of other stars, the observations of which have helped to define the envelope of possibilities for diffusion, mass loss, magnetic fields, etc. This progress has tended to increase our confidence in the SSM and its neutrino flux predictions.

It has also become clear that solar neutrinos play a unique role in particle physics. They may provide our only window on neutrino masses below 10^{-3} eV. In many extensions of the standard model this is the range of predicted masses. The unique sensitivity of solar neutrino experiments to new physics is due in great measure to the Mikheyev-Smirnov-Wolfenstein effect, the amplification of neutrino oscillations in matter [1,2].

The principal neutrino-producing reactions of the pp chain and CNO cycle are summarized in Table 1. The first six reactions produce β decay neutrino spectra having allowed shapes with endpoints given by E_ν^{max}. Deviations from an allowed spectrum occur for ^{8}B neutrinos because the ^{8}Be final state is a broad resonance [3]; much smaller deviations occur because of second-forbidden contributions to the decay. The last two reactions produce line sources of electron capture neutrinos, with widths $\sim$ 2 keV characteristic of the solar core temperature. The resulting solar neutrino spectrum is shown in Figure 1.

In the absence of new neutrino physics, measurements of the pp, ^{7}Be, and ^{8}B neutrino fluxes will determine the relative contributions of the ppI, ppII, and ppIII cycles that comprise the pp chain. As the discussion below will illustrate, the competition between the three cycles is governed in large classes of solar models by a single parameter, the central temperature T_c. The flux predictions of two standard models, those of Bahcall and Pinsonneault (BP) [4] and of Turck-Chièze and Lopez (TCL) [5], are included in Table 1.

1

Source	E_ν^{max} (MeV)	flux $(cm^{-2}s^{-1})$		
		BP(with diffusion)	BP(without)	TCL
$p+p\rightarrow^2H + e^+ + \nu$	0.42	6.00E10	6.04E10	6.03E10
$^{13}N\rightarrow^{13}C + e^+ + \nu$	1.20	4.92E8	4.35E8	3.83E8
$^{15}O\rightarrow^{15}N+e^+ + \nu$	1.73	4.26E8	3.72E8	3.18E8
$^{17}F\rightarrow^{17}O+e^+ + \nu$	1.74	5.39E6	4.67E6	
$^8B\rightarrow^8Be+e^+ + \nu$	~15	5.69E6	5.06E6	4.43E6
$^3He+p\rightarrow^4He+e^+ + \nu$	18.77	1.23E3	1.25E3	
$^7Be+e^- \rightarrow^7Li + \nu$	0.86(90%) 0.38(10%)	4.89E9	4.61E9	4.34E9
$p+e^-+p\rightarrow^2H+\nu$	1.44	1.43E8	1.43E8	1.39E8

Table 1: Neutrino fluxes predict by the Bahcall/Pinsonneault (with and without He diffusion) and Turck-Chiése/Lopes standard solar models.

§2 Experiment Results and SSM Uncertainties

Careful analyses of the experiments that will be described in Section 3 indicate that the observed solar neutrino fluxes differ substantially from SSM expectations [6,7,8]:

$$\phi(pp) \sim 0.9\,\phi^{SSM}(pp)$$
$$\phi(^7Be) \sim 0$$
$$\phi(^8B) \sim 0.43\,\phi^{SSM}(^8B). \qquad (1)$$

Reduced ^7Be and ^8B neutrino fluxes can be produced by lowering the central temperature of the sun somewhat. However, such adjustments, either by varying the parameters of the SSM or by adopting some nonstandard physics, tend to push the $\phi(^7Be)/\phi(^8B)$ ratio to higher values rather than the low one of Eq. (1),

$$\frac{\phi(^7Be)}{\phi(^8B)} \sim T_c^{-10}. \qquad (2)$$

Thus the observations seem difficult to reconcile with plausible solar model variations.

In order to assess how serious this problem is, several groups have considered the consequences of SSM uncertainties. These include the reaction cross sections for the pp chain and CNO cycle, the opacities, the deduction of heavy element abundances from solar surface abundances, the solar age and present day luminosity, and the equation of state. The astrophysical S factor for $^7Be(p,\gamma)^8B$ is among the most serious of the uncertainties, with different data sets allowing S(0) to range from approximately 20 to 25 eV barns; a recent measurement using a different technique, the breakup of ^8B in the Coulomb field of

^{208}Pb, has produced a preliminary central value of 16.7 ev barns [10]. There exist small differences in the BP and TCL SSMs in the treatments of $S_{33}(0)$, $S_{34}(0)$, the solar lifetime, plasma effects on Thompson scattering, and the composition, as well as in the error assigned to $S_{17}(0)$. Yet the sum of these differences affects the temperature-dependent $\phi(^8B)$ by less than 10%. In addition, the BP calculation differs from TCL by the inclusion of helium diffusion, which now is the largest contributor to the differences in the resulting flux predictions (12% in $\phi(^8B)$). (A recently updated BP calculation [4] also included the effects of metal diffusion.)

More important than the "best values" of the fluxes are the ranges that can be achieved by varying the parameters of the SSM within plausible bounds. In order to take into account the correlations among the fluxes when input parameters are varied, Bahcall and Ulrich [11] (BU) constructed 1000 SSMs by randomly varying five input parameters, the primordial heavy-element-to-hydrogen ratio Z/X and S(0) for the p-p, $^3He-^3He$, $^3He-^4He$, and p-^7Be reactions, assuming for each parameter a normal distribution with the mean and standard deviation used in their 1988 study. (These were the parameters assigned the largest uncertainties.) Smaller uncertainties from radiative opacities, the solar luminosity, and the solar age were folded into the results of the model calculations perturbatively, using [9] the partial derivatives of the BU SSM.

The resulting pattern of ^7Be and ^8B flux predictions is shown in Figure 2. The elongated error ellipses indicate that the fluxes are strongly correlated. Those variations producing $\phi(^8B)$ below $0.8\phi^{SSM}(^8B)$ tend to produce a reduced $\phi(^7Be)$, but the reduction is always less than 0.8.

Thus a greatly reduced $\phi(^7Be)$ cannot be achieved within the uncertainties assigned to parameters in the SSM.
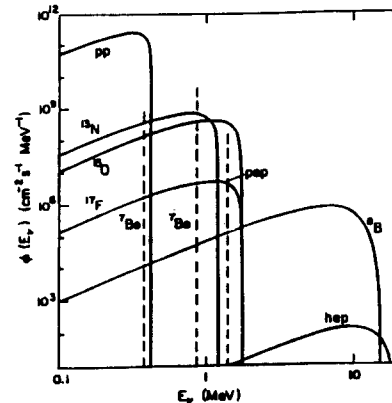

Figure 1: The flux densities (solid lines) of the principal β decay sources of solar neutrinos of the standard solar model. The total fluxes are those of the BP SSM. The ^7Be and pep electron capture neutrino fluxes (dashed lines) are discrete and given in units of $cm^{-2}s^{-1}$.

A similar exploration, but including parameter variations very far from their preferred values, was carried out by Castellani, Degl'Innocenti, Fiorentini, Ricci, and collaborators [12,13], who displayed their results as a function of the resulting core temperature T_c. The pattern that emerges is striking (see Figure 3): parameter variations producing the same value of T_c produce remarkably similar fluxes. Thus T_c provides an excellent one-parameter description of standard model perturbations. Figure 3 also illustrates the difficulty of producing a low ratio of $\phi(^7Be)/\phi(^8B)$ when T_c is reduced.

The BU 1000-solar-model variations were made under the constraint of reproducing the solar luminosity. Those variations show a similar strong correlation with T_c

$$\phi(pp) \propto T_c^{-1.2} \qquad \phi(^7Be) \propto T_c^8 \qquad \phi(^8B) \propto T_c^{18}. \qquad (3)$$

Figures 2 and 3 are a compelling argument that reasonable variations in the parameters of the SSM, or nonstandard changes in quantities like the metallicity, opacities, or solar age, cannot produce the pattern of fluxes deduced from experiment (Eq. (1)).

§3 The Detection Of Solar Neutrinos

Four solar neutrino experiments have now provided data, the Homestake ^{37}Cl experiment, the gallium experiments SAGE and GALLEX, and Kamiokande. The first three detectors are radiochemical, while Kamiokande records neutrino-electron elastic scattering event-by-event.
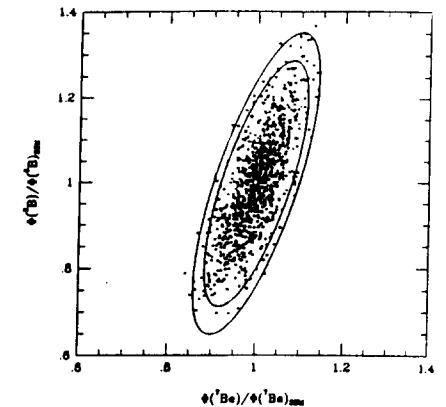

Figure 2: The dots represent the ^7Be and ^8B fluxes resulting from the 1000 SSMs of BU, with smaller SSM uncertainties added as in Ref. [9]. The 90 and 99% c.l. error ellipses are shown.

3.1 The Homestake Experiment

An experiment to detect neutrinos by the reaction $^{37}Cl(\nu_e,e)^{37}Ar$ has operated continuously in the Homestake Gold Mine since 1967 (apart from a 17 month hiatus in 1985/86 caused by the failure of the circulation pumps). The result of 25 years of measurement is [14]

$$(\sigma\phi)_{^{37}Cl} = 2.55 \pm 0.17 \pm 0.18 \quad SNU \qquad (1\sigma) \qquad (4)$$

which can be compared to the BP (with He diffusion) and TCL SSM predictions of 8.0 ± 1.0 SNU and 6.4 ± 1.4 SNU, respectively, all with 1σ errors. (One SNU = 10^{-36} captures/target atom/sec.) As we will discuss below, the ^8B and ^7Be contributions account for 77% (73%) and 15% (17%), respectively, of the BP (TCL) total. (Unless otherwise specified, BP refers to their 1992 results with He diffusion.)

The experiment [15,16] depends on the special properties of ^{37}Ar: as a noble gas, it can be removed readily

2   3

from perchloroethylene, while its half life ($\tau_{1/2} = 35$ days) allows both a reasonable exposure time and counting of the gas as it decays back to ^{37}Cl. Argon is removed from the tank by a helium purge, and the gas then circulated through a condensor, a molecular sieve, and a charcoal trap cooled to the temperature of liquid nitrogen. Typically $\sim 95\%$ of the argon in the tank is captured in the trap. (The efficiency is determined each run from the recovery results for a known amount of carrier gas, ^{36}Ar or ^{38}Ar, introduced into the tank at the start of the run.) When the extraction is completed, the trap is heated and swept by He. The extracted gas is passed through a hot titanium filter to remove reactive gases, and then other noble gases are separated by gas chromatography. The purified argon is loaded into a small proportional counter along with tritium-free methane, which serves as a counting gas. Since the electron capture decay of ^{37}Ar leads to the ground state of ^{37}Cl, the only signal for the decay is the 2.82 keV Auger electron produced as the atomic electrons in ^{37}Cl adjust to fill the K-shell vacancy. The counting of the gas typically continues for about one year (~ 10 half lives).
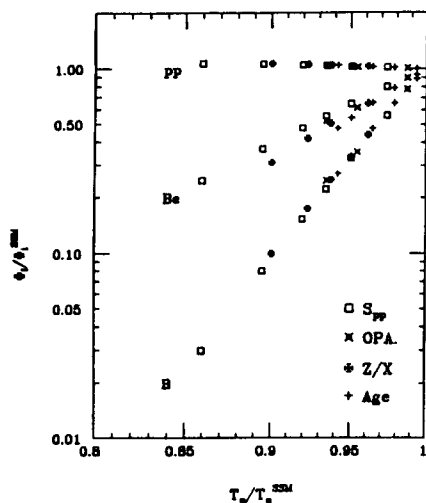
Figure 3: The response of the pp, Be, and ^{8}B fluxes to the indicated variations in solar model input parameters, displayed as a function of the resulting central temperature T_c. From Castellani, Degl'Innocenti, Fiorentini, Lissia, and Ricci [12].

The measured cosmic ray-induced background in the Homestake detector is 0.06 ^{37}Ar atoms/day while neutron-induced backgrounds are estimated to be below 0.03 atoms/day. A signal of 0.48 ± 0.04 atoms/day is attributed to solar neutrinos. When detector efficiencies, ^{37}Ar decays occurring in the tank, etc., are taken into account, the number of ^{37}Ar atoms counted is about 25/year.

A variety of careful tests of the argon recovery and counting efficiency have been made over the past 25 years. For example, it has been verified that ^{37}Ar produced in the tank by a fast neutron source, which induces (n,p) reactions followed by (p,n) on ^{37}Cl, is quantitatively recovered. Tests have also been made of the recovery of ^{36}Ar produced by the decay of long-lived ^{36}Cl in perchloroethylene. The experiment, performed in a tightly sealed tank to prevent contamination from air inleakage, resulted in a yield of 100 ± 3%. However, the detector has never been calibrated directly with a neutrino source, despite studies of the feasibility of a ^{65}Zn source [17].

The significance of the Homestake results is due in part to an accurately determined ^{37}Cl cross section. As the 814 keV threshold for exciting the ^{37}Ar ground state is above the pp endpoint, the detector is sensitive primarily to ^{7}Be and ^{8}B neutrinos (see Table 2). The cross section for ^{7}Be neutrinos (and the weaker fluxes of pep and CNO cycle neutrinos) is determined by the known half life of ^{37}Ar. However, ^{8}B neutrinos can generate transitions to many excited states below the particle breakup threshold in ^{37}Ar. The superallowed transition to the 4.99 MeV state, dominated by the Fermi matrix element of known strength, accounts for about 60% of the SSM cross section. The allowed transition strengths can be measured by observing the delayed protons following the β decay of ^{37}Ca, the isospin analog of the reaction ^{37}Cl(ν_e,e) ^{37}Ar [18]. While it was believed that this measurement had been properly done many years ago, the issue was not resolved until kinematically complete measurements were done recently [19,20]. The net result is a ^{37}Cl cross section believed to be accurate to about 3%.

3.2 The Kamiokande Experiment

The Kamiokande experiment [21,22] is a 4.5 kiloton cylindrical imaging water Cerenkov detector originally designed for proton decay searches, but later reinstrumented to detect low energy neutrinos. It detects neutrinos by the Cerenkov light produced by recoiling electrons in the reaction

$$\nu_x + e \rightarrow \nu_x' + e'. \quad (5)$$

Both ν_e and heavy flavor neutrinos contribute, with $\sigma(\nu_e)/\sigma(\nu_\mu) \sim 7$. The inner volume of 2.14 kilotons is viewed by 948 Hamamatsu 20" photomultiplier tubes

(PMTs) providing 20% photocathode coverage, and the surrounding 1.5m of water, serving as an anticounter, is viewed by 123 PMTs. The fiducial volume for solar neutrino measurements is the central 0.68 kilotons of water, the detector region most isolated from the high energy gamma rays generated in the surrounding rock walls of the Kamioka mine.
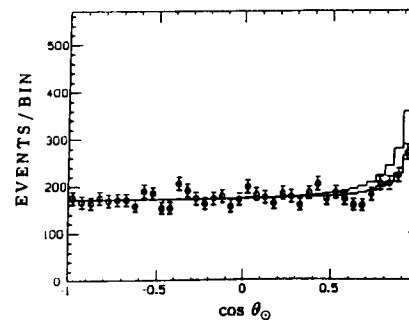
Figure 4: Angular distribution of recoil electrons from Kamiokande II and III showing the excess at forward angles that is attributed to solar neutrinos. Electrons with apparent energies between 7 and 20 MeV are included. The upper histogram is the SSM prediction of BU superimposed on an isotropic background, while the lower histogram is the best fit. From K. Nakamura [24].

In the conversion of the original proton decay detector to Kamiokande, great effort was invested in reducing low energy backgrounds associated with radon and uranium. This included sealing the detector against radon inleakage and recirculating the water through ion exchange columns. The relatively shallow depth of the Kamioka mine (2700 m.w.e.) leads to an appreciable flux of cosmic ray muons which, on interacting with ^{16}O, produce various short-lived spallation products. These β decay activities are vetoed by their correlation in time with the muons. The experimenters succeeded in lowering the detector threshold to 9 MeV and later to 7.5 MeV. Kamiokande III included improvements in the electronics and the installation of wavelength shifters around the PMTs to increase light collection and currently operates with a threshold of 7.0 MeV.

Kamiokande II/III detects the high energy portion of the ^{8}B neutrino spectrum. Between December, 1985, and July, 1993, 1667 live detector days of data were accumulated. Under the assumption that the incident neutrinos are ν_es with an undistorted ^{8}B β decay spectrum, the

combined Kamiokande II/III data set gives [23,24]

$$\phi_{\nu_e}(^8\text{B}) = (2.89 \pm 0.22 \pm 0.35) \cdot 10^6/cm^2 s \quad (1\sigma) \quad (6)$$

corresponding to 51% of the BP and 65% of the TCL SSM predictions. The total number of detected solar neutrino events is 476^{+36}_{-34}.

This experiment is remarkable in several respects. It is the first detector to measure solar neutrinos in real time. Essential to the experiment is the sharp peaking of the electron angular distribution in the direction of the incident neutrino: this forward peaking, illustrated in Figure 4, allows the experimenters to separate solar neutrino events from an isotropic background. The unambiguous observation of a peak in the cross section correlated with the position of the sun is the first direct demonstration that the sun produces neutrinos as a byproduct of fusion. Finally, although reaction (5) is a soft process where the recoil electron and scattered neutrino share the initial energy, the recoil electron energy distribution provides some information on the incident neutrino spectrum. The recoil spectrum measured by Kamiokande II/III is consistent with an allowed ^{8}B incident neutrino spectrum, with the overall flux reduced as in Eq. (6). However the statistical accuracy is not high.

3.3 The SAGE and GALLEX Experiments

Two radiochemical gallium experiments exploiting the reaction ^{71}Ga(ν_e,e)^{71}Ge, SAGE and GALLEX, began solar neutrino measurements in January, 1990, and May, 1991, respectively. SAGE operates in the Baksan Neutrino Observatory, under 4700 m.w.e. of shielding from Mount Andyrchi in the Caucasus, while GALLEX is housed in the Gran Sasso Laboratory at a depth of 3300 m.w.e. These experiments are sensitive primarily to the low-energy pp neutrinos, the flux of which is sharply constrained by the solar luminosity in any steady-state model of the sun (see Table 2). The gallium experiment was first suggested by Kuzmin [25]. In 1974 Ray Davis and collaborators began work to develop a practical experimental scheme. Their efforts, in which both GaCl$_3$ solutions and Ga metal targets were explored, culminated with the 1.3-ton Brookhaven/Heidelberg/Rehovot/Princeton pilot experiment in 1980-82 that demonstrated the procedures later used by GALLEX [26].

The primary obstacles to mounting the gallium experiments were the cost of the target and the greater complexity of the ^{71}Ge chemical extraction. The GALLEX experiment [27,28] employs 30 tons of Ga as a solution of GaCl$_3$ in hydrochloric acid. After an exposure of about three weeks, the Ge is recovered as GeCl$_4$ by bubbling nitrogen through the solution and then scrubbing the gas through a water absorber. The Ge is further concentrated

4

5

and purified, and finally converted into GeH_4 which, when mixed with Xe, makes a good counting gas. The overall extraction efficiency is typically 99%. The GeH_4 is inserted into miniaturized gas proportional counters, carefully designed for their radiopurity, and the Ge counted as it decays back to Ga ($\tau_{1/2} = 11.43$ d). As in the case of ^{37}Ar, the only signal for the Ge decay is the energy deposited by Auger electrons and x-rays that accompany the atomic rearrangement in Ga. An important achievement of GALLEX has been the detection of both the K peak (10.4 keV) and L peak (1.2 keV). While 88% of the electron captures occur from the K shell, many of the subsequent $K \rightarrow L$ x-rays escape the detector and some of the Auger electrons hit the detector walls. This produces a shift of the detected energy of events from the K to the L and M peaks. Thus the GALLEX L-peak counting capability almost doubles the ^{71}Ge detection efficiency.

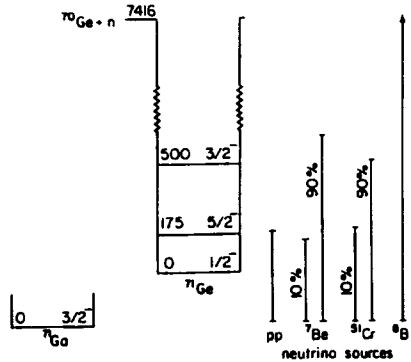Figure 5: Level scheme for ^{71}Ge showing the excited states that contribute to absorption of pp, ^7Be, ^{51}Cr, and ^8B neutrinos. The $^{70}Ge + n$ break-up threshold is 7.4 MeV.

Gallium, like mercury, is a liquid metal at room temperature. SAGE [29,30] uses metallic gallium as a target, separating the ^{71}Ge by vigorously mixing into the gallium a mixture of hydrogen peroxide and dilute hydrochloric acid. This produces an emulsion, with the Ge migrating to the surface of the emulsion droplets where it is oxidized and dissolved by hydrochloric acid. The Ge is extracted as $GeCl_4$, purified and concentrated, synthesized into GeH_4, and further purified by gas chromatography. The overall efficiency, determined by introducing a Ge carrier, is typically 80%. The Ge counting proceeds as in GALLEX.

SAGE began operations with 30 tons of gallium, and now operates with 55 tons. The combined result for stage I (prior to September, 1992) and the first nine runs of stage II (9/92 - 6/93) is [31]

$$(\sigma\phi)_{^{71}Ge} = 69^{+11}_{-11}\,(stat)^{+6}_{-7}\,(sys)\ SNU \quad (1\sigma). \quad (7)$$

This result includes only events counted in the K peak. The counter and electronics improvements made at the start of stage II should permit L-peak events to be included, but no results have been announced as of December, 1994. The corresponding results for GALLEX I (first 15 runs) and II (8/92-10/93) is [27]

$$(\sigma\phi)_{^{71}Ge} = 79 \pm 10 \pm 6\ SNU \quad (1\sigma). \quad (8)$$

GALLEX II solar neutrino runs continued until June, 1994, but results for the last portion of this period have not been reported.

GALLEX II solar neutrino runs were interrupted in June, 1994, to permit an overall test of the detector with a ^{51}Cr source, which produces line sources of 746 keV (90%) and 426 keV (10%) neutrinos. The 1.67 MCi source was produced by irradiating ~ 36 kg of chromium, enriched in ^{50}Cr, in the Siloé reactor in Grenoble. Following exposure of the detector and recovery and counting of the produced ^{71}Ge, the ratio of measured ^{71}Ge to expected was calculated [32],

$$R = 1.04 \pm 0.12 \quad (1\sigma). \quad (9)$$

This is the first test of a solar neutrino detector with an terrestrial, low energy neutrino source. A similar source (~ 0.5 MCi) has been produced by the SAGE collaboration and was installed in their detector in December, 1994 (J.F. Wilkerson, private communication). The higher Ga density of the SAGE detector increases the effectiveness of the source by about a factor of 2.5, helping to compensate for the weaker neutrino flux.

The nuclear physics of the reaction $^{71}Ga(\nu_e,e)^{71}Ge$ is illustrated in Figure 5. As the threshold is 233 keV, the ground state and first excited state can be excited by pp neutrinos. However, as only those pp neutrinos within 12 keV of the endpoint can reach the excited state, the phase space for reaching this state is smaller by a factor of ~ 100. Thus the cross section is determined precisely by the measured electron capture lifetime of ^{71}Ge. In the BP and TCL calculations these neutrinos account for 54% and 57% of the capture rate, respectively, each predicting 71 SNU. Because of this strong pp neutrino contribution, there exists a minimal astronomical counting rate of 79 SNU [33] for the Ga detector that assumes only a steady-state sun and standard model weak interaction physics. This minimum value corresponds to a sun that produces the observed luminosity entirely through the ppI cycle. The rates found by SAGE and GALLEX are quite close to this bound.

The ^7Be neutrinos can excite the ground state and two excited states at 175 keV ($5/2^-$) and 500 keV ($3/2^-$). The source experiment was important not only in checking the overall efficiency of the Ga chemistry, but also in restricting the contributions of the excited states to ^7Be capture. As the SSM ^7Be capture rates of BP and TCL are both above 30 SNU, the SAGE/GALLEX results alone suggest some reduction in the low-energy pp and ^7Be fluxes.

The ^8B neutrino capture rates (14 and 11 SNU in the BP and TCL SSMs, respectively) have been calculated from the GT profile deduced by Krofcheck et al. [35]. The corresponding total SSM rates for this detector are 132 SNU and 123 SNU (see Table 2).
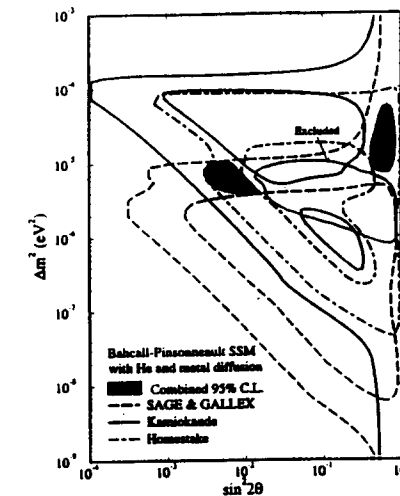

Figure 6: The MSW solutions allowed at 95% c.l. by the combined results of the Homestake, SAGE/GALLEX, and Kamiokande experiments, including Kamiokande II day-night constraints and the GALLEX source experiment results, for the BP flux predictions with He and metal diffusion. From Hata and Haxton [34].

§4 Particle Physics Solutions

In Section 2 it was shown that solar models which reduce the high energy neutrino flux tend to enhance the $^7Be/^8B$ flux ratio, contradicting the results of the Homestake, SAGE/GALLEX, and Kamiokande experiments.

An alternative solution, physics beyond the standard model of electroweak interactions, would have far-reaching consequences. Particle physics solutions of the solar neutrino problem include neutrino oscillations, neutrino decay, neutrino magnetic moments, and weakly interacting massive particles. Among these, the Mikheyev-Smirnov-Wolfenstein effect — neutrino oscillations enhanced by matter interactions — is widely regarded as the most plausible.

Neither Dirac nor Majorana neutrino masses can be generated in the standard electroweak model, which contains no right-handed neutrino fields and has only a doublet scalar field. However both neutrino masses and flavor mixing are expected in most extensions of this model. In the seesaw mechanism light neutrinos with $m_{light} \sim \frac{m_D^2}{m_R}$ arise, where m_D is a familiar Dirac mass (often a quark mass m_u, m_c, or m_t) and m_R a heavy right-handed Majorana mass. Taking $m_R \sim 10^{16}$ GeV, a typical grand unification scale for models built on groups like SO(10), the seesaw mechanism gives the crude relation

$$m_{\nu_e} : m_{\nu_\mu} : m_{\nu_\tau} \leftrightarrow 2\cdot 10^{-12} : 2\cdot 10^{-7} : 3\cdot 10^{-3} eV. \quad (10)$$

The fact that solar neutrino experiments can probe small neutrino masses, and thus provide insight into possible new mass scales m_R that are far beyond the reach of direct accelerator measurements, has been an important theme of the field.

Flavor mixing of massive neutrinos leads to neutrino oscillations: the probability that a ν_e will remain a ν_e after propagating a distance x is

$$P_{\nu_e}(x) = 1 - \sin^2 2\theta_v \sin^2\left(\frac{\delta m^2 x}{4E}\right) \xrightarrow{x\to\infty} 1 - \frac{1}{2}\sin^2 2\theta_v \quad (11)$$

where E is the neutrino energy, $\delta m^2 = m_2^2 - m_1^2$, and θ_v the vacuum mixing angle. If the oscillation length

$$L_o = \frac{4\pi E}{\delta m^2} \quad (12)$$

is comparable to or shorter than one astronomical unit, a reduction in the ν_e flux would be expected in solar neutrino experiments. The suggestion that the solar neutrino problem could be explained by neutrino oscillations was first made by Pontecorvo [36], who pointed out the analogy with $K_0 \leftrightarrow \bar{K}_0$ oscillations. From the point of view of particle physics, the sun is a marvelous neutrino source. The neutrinos travel a long distance and have low energies (~ 1 MeV), implying a sensitivity to

$$\delta m^2 \gtrsim 10^{-12} eV^2. \quad (13)$$

In the seesaw mechanism, $\delta m^2 \sim m_2^2$, so neutrino masses as low as $m_2 \sim 10^{-6}$ eV could be probed. In contrast, terrestrial oscillation experiments with accelerator or reactor neutrinos have been typically limited to $\delta m^2 \gtrsim 0.1 eV^2$.

neutrino source	capture rates (SNU)			
	^{37}Cl(BP)	^{37}Cl(TCL)	^{71}Ga(BP)	^{71}Ga(TCL)
pp	0.0	0.0	70.8	71.1
pep	0.2	0.22	3.1	2.99
^{7}Be	1.2	1.10	35.8	30.9
^{8}B	6.2	4.63	13.8	10.77
^{13}N	0.1	0.063	3.0	2.36
^{15}O	0.3	0.21	4.9	3.66
Total	8.0	6.36	131.5	122.5

Table 2: Predicted capture rates in SNU of the BP and TCL SSMs for the ^{37}Cl and SAGE/GALLEX experiments.

From Eq. (11) one expects vacuum oscillations to affect all neutrino species equally, if the oscillation length is small compared to an astronomical unit. This appears to contradict observation, as the pp flux may not be significantly reduced. Furthermore, the theoretical prejudice that θ_v should be small makes this an unlikely explanation of the significant discrepancies with SSM ^{7}Be and ^{8}B flux predictions.

The first objection, however, can be circumvented in the case of "just so" oscillations where the oscillation length is comparable to one astronomical unit [37]. In this case the oscillation probability becomes sharply energy dependent, and one can choose δm^2 to preferentially suppress one component (e.g., the monochromatic ^{7}Be neutrinos). This scenario has been explored by several groups and remains an interesting possibility. However, the requirement of large mixing angles remains.

The community's view of neutrino oscillations as a solution of the solar neutrino problem changed dramatically when Mikheyev and Smirnov [1,2] showed that the density dependence of the neutrino effective mass, a phenomenon first discussed by Wolfenstein [38], could greatly enhance oscillation probabilities. If the ν_e is primarily comprised of the light eigenstate in vacuum with the ν_μ being heavier, a critical density exists where the matter effects compensate for the vacuum mass difference. This comes about because of the stronger matter interactions of the ν_e, which scatters off solar electrons by both charged and neutral current interactions. Consequently a ν_e produced at sufficiently high densities in the core will be the heavy eigenstate in medium. If it then adiabatically propagates to the solar surface, it will emerge as the heavy eigenstate in vacuum, i.e., primarily a ν_μ. This phenomenon has been investigated numerically by a number of groups. (See, e.g., Rosen and Gelb [39].)

The resulting MSW fit to the ^{37}Cl, Kamiokande, and SAGE/GALLEX experiments, including the constraints from the recent GALLEX neutrino source experiment [32], is shown in Figure 6 [34]. The calculation includes the (correlated) theoretical uncertainties in the SSM flux predictions, terrestrial regeneration, the Kamiokande day-night data, and an improved definition of confidence level contours (see Hata and Langacker [8]). The preferred (in the sense of minimizing the χ^2) solution corresponds to a region surrounding $\delta m^2 \sim 6 \cdot 10^{-6} \text{eV}^2$ and $\sin^2 2\theta_v \sim 6 \cdot 10^{-3}$. It is commonly called the small-angle solution. A second, large-angle solution exists, corresponding to $\delta m^2 \sim 10^{-5} \text{eV}^2$ and $\sin^2 2\theta_v \sim 0.6$, but this region of Figure 6 has shrunk as the precision of the gallium experiments improve.

These solutions can be distinguished by their characteristic distortions of the solar neutrino spectrum. The survival probabilities $P_{\nu_e}^{MSW}(E)$ for the small- and large-angle parameters given above are shown as a function of E in Figure 7.

The calculations of Figure 6 assume flavor oscillations into a ν_μ or ν_τ. This influences the interpretation of the Kamiokande experiment, as heavy flavor neutrinos contribute to elastic scattering. Another possibility is an oscillation into a sterile neutrino. The large-angle solution is then ruled out by the Kamiokande requirement of a large ν_e survival probability.

The MSW mechanism provides a natural explanation for the pattern of observed solar neutrino fluxes. While it requires profound new physics, both massive neutrinos and neutrino mixing are expected in extended models. The preferred solutions correspond to $\delta m^2 \sim 10^{-5} \text{ eV}^2$, and thus are consistent with $m_2 \sim$ few $\cdot 10^{-3}$ eV. This is a typical ν_τ mass in models where $m_R \sim m_{GUT}$. On the other hand, if it is the ν_μ participating in the oscil-

lation, this gives $m_R \sim 10^{12}$ GeV and predicts a heavy seesaw $\nu_\tau \sim 10$ eV [40]. Such a mass is of great interest cosmologically as it would have consequences for supernova neutrinos [41,42], the dark matter problem, and the formation of large-scale structure.

If the MSW mechanism proves not to be the solution of the solar neutrino problem, it still will have greatly enhanced the importance of solar neutrino physics: the existing experiments have ruled out large regions in the $\delta m^2 - \sin^2 2\theta_v$ plane (corresponding to nearly complete $\nu_e \to \nu_\mu$ conversion) that remain hopelessly beyond the reach of accelerator neutrino oscillation experiments.

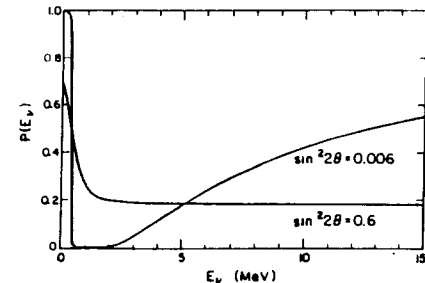Figure 7: MSW survival probabilities $P_{\nu_e}^{MSW}(E)$ for typical small-angle ($\delta m^2 \sim 6 \cdot 10^{-6} \text{eV}^2, \sin^2 2\theta_v \sim 6 \cdot 10^{-3}$) and large-angle ($\delta m^2 \sim 10^{-5} \text{eV}^2, \sin^2 2\theta_v \sim 0.6$) solutions.

§5 New Experiments

The MSW mechanism has had a particularly strong impact because it was discovered at a time when new data (SAGE/GALLEX, Kamiokande, helioseismology) were eliminating many competing solutions to the solar neutrino problem. The physics of the MSW mechanism is both simple and elegant, which accounts for much of its appeal. But the most important attribute of this solution is that it can be definitively tested. The favored small-angle solution produces a distinctive distortion in the solar neutrino spectrum. Furthermore, if the oscillation is into another flavor (rather than a sterile state), the missing neutrinos can be found through their neutral current interactions. These tests will be made by two high-statistics, direct-counting directors now under construction.

5.1 The Sudbury Neutrino Observatory

A water Cerenkov detector of a different type is under construction deep (5900 m.w.e.) within the Creighton #9

nickel mine at Sudbury, Ontario, Canada [43,44,45]. The central portion of the detector is an acrylic vessel containing 1 kiloton of heavy water, D_2O. This is surrounded by five meters of light water to protect the inner detector from neutrons and gammas. The detector is viewed by 9500 20-cm PMTs, providing 56% photocathode coverage (Figure 8).

The D_2O introduces two new channels. The charged current breakup reaction

$$\nu_e + D \to p + p + e^-$$
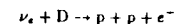
produces a recoil electron which carries off almost all of the final-state kinetic energy. As the Gamow-Teller strength is concentrated very close to the p+p threshold, 1.44 MeV, the electron and neutrino energies are related by $E_\nu \sim E_e + 1.44$ MeV. Thus, neutrino spectrum distortions should show up clearly in the measured electron energy distribution. As the GT strength in the deuteron is equivalent to about one-third of a free neutron, the anticipated counting rates are high. For an electron detection threshold of 5 MeV and a ^{8}B neutrino flux equal to about 50% of the BP SSM value, 3300 events will be recorded each year.

A second channel is sensitive equally to neutrinos of any flavor,

$$\nu_x + D \to \nu_x' + n + p$$
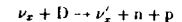
and thus will be crucial in testing whether flavor oscillations have occurred. The anticipated event rate is approximately 2000/year in the BP SSM. The addition of $MgCl_2$ to the D_2O at a concentration of 0.2-0.3% allows the neutrons to be observed by ^{35}Cl(n,γ). The Cerenkov light produced by the showering of the 8.6 MeV capture γ ray will add to the signal from the charged current reaction. By operating the detector with and without salt, the experimenters will separate the charged and neutral current signals. The SNO collaboration also plans to deploy proportional counters filled with ^{3}He to exploit the neutron-specific charge-exchange reaction ^{3}He(n,p)^{3}H. With such detectors, SNO will be sensitive to neutral current events at all times.

The detection of ~ 8 neutrons/day in a kiloton detector places extraordinary constraints on radiopurity. For example, a potentially serious background source is the photodisintegration of deuterium by energetic photons from U and Th chains. The experimental goal is concentrations of $\lesssim 10^{-14}$ grams of U and Th per gram of D_2O.

SNO is scheduled to begin operations late in 1996.

5.2 Superkamiokande

Superkamiokande will be a greatly enlarged version of Kamiokande II/III with improved threshold (5 MeV) and energy and position resolution [46,47,48]. It is currently

under construction in the Kamioka mine at a depth of 2700 m.w.e.

The fiducial volume for detecting solar neutrinos will be 22 kilotons, compared to 0.68 kilotons in the existing detector. This plus the improved threshold will increase the detection rate for neutrino-electron scattering by a factor of ~ 90, to 8400/year. Despite the soft kinematics of the $\nu_e - e$ reaction, the experimenters believe the high statistics will allow them to distinguish the spectral distortions produced by competing MSW solutions.
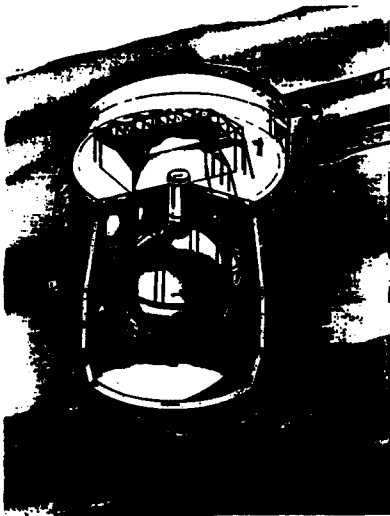

Figure 8: Schematic of the SNO detector now under construction in the Creighton #9 nickel mine, Sudbury. Provided by R.G.H. Robertson and J.F. Wilkerson (private communication).

Because elastic scattering is sensitive to both ν_e and heavy-flavor neutrinos (in the ratio of 7:1), an accurate SNO determination of the ν_e spectrum will allow SuperKamiokande to extract the spectrum of $\nu_\mu s$ or $\nu_\tau s$.

SuperKamiokande construction is scheduled to be completed in mid 1996.

5.3 Other Future Detectors

The Borexino collaboration [49,50] has proposed a 0.3 kiloton liquid scintillator for installation in the Gran Sasso Laboratory. The experimenters hope to detect ^{7}Be neu-

trinos by $\nu - e$ scattering. The detection of very low energy recoil electrons places stringent constraints on U, Th, K, and other activities in the detector, e.g., $\lesssim 10^{-16}$ g U/g, including a requirement for continuous purification. The experimenters will evaluate background problems in a test facility now under construction, and scheduled to be completed by the end of 1995. The anticipated counting rate for the full-scale detector is $\sim 18,000$ ^{7}Be neutrino events/year for the BP SSM.

A high-counting-rate twin of the ^{37}Cl detector utilizing the reaction ^{127}I$(\nu_e,e)^{127}$Xe has been funded recently and is under construction in the Homestake mine [51,52]. With a threshold of 664 keV, the detector is primarily sensitive to ^{7}Be and ^{8}B neutrinos. The initial Homestake detector will contain 100 tons of iodine as a solution of NaI. A smaller version of this detector was recently used at the LAMPF beamstop to measure the ^{127}I cross section for stopped muon decay $\nu_e s$. Calibration of the ^{7}Be neutrino cross section by an ^{37}Ar neutrino source is also planned. The 100-ton detector is scheduled to be completed by the end of 1995, with plans for an expansion to 1 kiloton afterwards.

A 5-kiloton liquid argon time projection chamber, ICARUS II, has been proposed for Gran Sasso [53]. In addition to $\nu - e$ scattering, the charged current channel

$$\nu_e + {}^{40}\text{Ar} \rightarrow e^- + {}^{40}\text{K}^*$$
$$\hookrightarrow {}^{40}\text{K} + \gamma$$
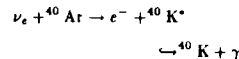
will allow the experimenters to measure the shape of the high-energy portion of the ^{8}B ν_e spectrum.

There are a number of important development efforts underway that focus on new technologies for the next generation of solar neutrino detectors. Some of the significant challenges motivating these efforts include neutrino detection by coherent scattering off nuclei and real-time detectors for pp neutrinos, such as the superfluid ^{4}He detector HERON [54] and the high-pressure helium time projection chamber HELLAZ [55].

§6   OUTLOOK

The successes of the Kamiokande and SAGE/GALLEX experiments have led to a more complicated solar neutrino problem. The apparent strong suppression of the ^{7}Be flux (negative in most unconstrained fits!) has led many to conclude that a particle physics solution such as the MSW mechanism is likely.

An MSW solution to the solar neutrino problem would have deep implications for particle physics and cosmology. The most important aspect of this candidate solution is that it can be tested experimentally. The presence of a heavy-flavor solar neutrino component and spectral distortions will be probed by SNO and SuperKamiokande.

If these experiments indicate neutrino oscillations, enormous attention will then be focused on this field. It will be imperative to measure the flux, flavor, and spectral distribution of the ^{7}Be and pp neutrinos in order to exploit this unique window on physics beyond the standard electroweak model.

Under any scenario, one must appreciate the difficulty of the current generation of experiments. For example, the radiopurity goals of SNO and SuperKamiokande are unprecedented. It is therefore important to support a variety of experiments, so that some cross checks on the results are available. In view of the implications these experiments may have, the physics community will demand redundancy.

There are exciting new technologies under development that should be encouraged. These developmental efforts will lead to the detectors of the next decade. There are excellent ideas for active detectors sensitive to pp neutrinos. Cryogenic technologies could lead to low-threshold detectors exploiting coherent scattering.

The progress that has been made in recent years is remarkable: three new experiments have yielded data, and the extraordinary potential of the sun to enhance flavor oscillations is understood. The SNO and SuperKamiokande detectors are nearing completion, and new efforts on Borexino and the iodine detector are underway. Clearly this vital field is on the threshold of new discoveries.

§References

[1] S.P. Mikheyev, A. Yu. Smirnov, *Sov. J. Nucl. Phys.* 42 (1985) 913-7.

[2] S.P. Mikheyev, A. Yu. Smirnov, *Nuovo Cimento*, 9C (1986) 17-26.

[3] J.N. Bahcall, B.R. Holstein, *Phys. Rev. C* 33 (1986) 2121-7.

[4] J.N. Bahcall, M.H. Pinsonneault, *Rev. Mod. Phys.* 64 (1992) 885-926; An updated calculation that includes the effects of metal diffusion is: J.N. Bahcall, M.H. Pinsonneault, 1995. To appear in *Rev. Mod. Phys*.

[5] S. Turck-Chièze, I. Lopez, *Ap. J.* 408 (1993) 347-67.

[6] M. White, L. Krauss, E. Gates, *Phys. Rev. Lett.* 70 (1993) 375-8.

[7] S.J. Parke, *Phys. Rev. Lett.* 74 (1995) 839-41; W. Kwong and S.P. Rosen, *Phys. Rev. Lett.* 73 (1994) 369.

[8] N. Hata, P. Langacker, *Phys. Rev. D.* 48 (1994) 2937-40.

[9] J.N. Bahcall, W.C. Haxton, *Phys. Rev. D.* 40 (1989) 931-41.

[10] T. Motobayashi, N. Iwasa, Y. Ando, M. Kurokawa, H. Murakami, et al., *Phys. Rev. Lett.* 73 (1994) 2680-3.

[11] J.N. Bahcall, R.K. Ulrich, 1988. *Rev. Mod. Phys.* 60 (1988) 297-372.

[12] V. Castellani, S. Degl'Innocenti, G. Fiorentini, M. Lissia, B. Ricci, *Phys. Rev. D.* 50 (1994) 4749-61.

[13] V. Castellani, S. Degl'Innocenti, G. Fiorentini, B. Ricci, In *Proc. Solar Modeling Workshop*, ed. A.B. Balantekin, J.N. Bahcall, (1995) Singapore: World Scientific, in press

[14] K. Lande, In *Neutrino '94*, ed. A. Dar, G. Eilam, M. Groneau, (1995) Amsterdam: North Holland.

[15] R. Davis Jr., In *Solar Neutrinos and Neutrino Astronomy*, ed. M.L. Cherry, W.A. Fowler, K. Lande. New York: American Institute of Physics, (1985) pp 1-21.

[16] R. Davis Jr., In *Frontiers of Neutrino Astrophysics*, ed. Y Suzuki and K Nakamura 47 (1993) University Academy Press.

[17] L.W. Alvarez, *Lawrence Radiation Lab. Physics Notes*, (1973) memo #767.

[18] J.N. Bahcall, *Phys. Rev. Lett.* 17 (1966) 398-401.

[19] A. Garcia, E.G. Adelberger, P.V. Mangus, H.E. Swanson, H.E. Tengblad, et al., *Phys. Rev. Lett.* 67 (1991) 3654-7.

[20] A. Garcia, E.G. Adelberger, P.V. Mangus, H.E. Swanson, D.P. Wells, et al., *Phys. Rev. C* 51 (1995) R439-42.

[21] K.S. Hirata, T. Kajita, M. Koshiba, M. Nakahata, Y. Oyama, et al., *Phys. Rev. D.* 38 (1988) 448-58.

[22] K.S. Hirata, K. Inoue, T. Ishida, T. Kajita, K. Kihara, et al., *Phys. Rev. D.* 44 (1991) 2241-60.

[23] Y. Suzuki, in *Proc. 16th Int. Conf. on Neutrino Physics and Astrophysics*, to be published (1995).

[24] K. Nakamura, To be published in *Proc. Int. Conf. on Non-Accelerator Particle Physics* (1994) (India).

[25] V.A. Kuzmin, *Sov. Phys. JETP*, 22 (1966) 1051; V.A. Kuzmin, G.T. Zatsepin, *Proc. Int. Conf. on Cosmic Rays* 2 (1966) 1023.

[26] W. Hampel, In *Solar Neutrinos and Neutrino Astronomy*, ed. M.L. Cherry, W.A. Fowler, K. Lande. New York: American Institute of Physics, (1985) pp. 162-74.

[27] P. Anselmann, W. Hampel, G. Heusser, J. Kiko, T. Kirsten, et al., *Phys. Lett. B*. 285 (1992) 376-89.

[28] P. Anselmann, W. Hampel, G. Heusser, J. Kiko, T. Kirsten, et al., *Phys. Lett. B*. 327 (1994) 377-85.

[29] J.N. Abdurashitov, E.L. Faizov, V.N. Gavrin, A.O. Gusev, A.V. Kalikov, et al., *Phys. Lett. B*. 328 (1994) 234-48.

[30] T.J. Bowles, V.N. Gavrin, *Annu. Rev. Nucl. Part. Sci.* 43 (1993) 117-64.

[31] J.S. Nico, In *Neutrino '94*, ed. A. Dar, G. Eilam, M. Groneau, Amsterdam: North Holland and talk presented at the *Int. Conf. High Energy Physics*, (1995) Glasgow.

[32] P. Anselmann, R. Frockenbrock, W. Hampel, G. Heusser, J. Kiko, et al., *Phys. Lett. B*. 342 (1995) 440-50.

[33] J.N. Bahcall, *Neutrino Astrophysics*, Cambridge: Cambridge Univ. Press. (1989) 567 pp.

[34] N. Hata, W.C. Haxton, To appear in *Phys. Lett. B*. (1995).

[35] D. Krofcheck, E. Sugarbaker, J. Rapaport, D. Wang, J.N. Bahcall, et. al., *Phys. Rev. Lett.* 55 (1985) 1051-4; D. Krofcheck, Ph.D. thesis, (1987) Ohio State University.

[36] B. Pontecorvo, *Sov. Phys. JETP*. 7 (1958) 172.

[37] S.L. Glashow, L.M. Krauss, *Phys. Lett. B*. 190 (1987) 199-207.

[38] L. Wolfenstein, 1978. *Phys. Rev. D*. 17 (1978) 2369-74; *Phys. Rev. D*. 20 (1979) 2634-35.

[39] S.P. Rosen and J.M. Gelb, *Phys. Rev. D*. 34 (1986) 969-79.

[40] S.A. Bludman, D.C. Kennedy, P.G. Langacker, *Phys. Rev. D*. 45 (1992) 1810-13.

[41] G.M. Fuller, R.W. Mayle, B.S. Meyer, J.R. Wilson, *Ap. J.* 389 (1992) 517-526.

[42] Y.Z. Qian, F.M. Fuller, R. Mayle, G.J. Mathews, J.R. Wilson, S.E. Woosley, *Phys. Rev. Lett.* 71 (1993) 1965-8.

[43] G.T. Ewan, H.C. Evans, H.W. Lee, J.R. Leslie, H.B. Mak, et al., (1987) Queen's University report SNO-87-12.

[44] G. Aardsma, R.C. Allan, J.D. Anglin, M. Bercovitch, A.L. Carter, et al., *Phys. Lett. B*. 194 (1987) 321-25.

[45] H.H. Chen, *Phys. Rev. Lett.* 55 (1985) 534-6.

[46] Y. Totsuka, In *Proc. 7th Workshop on Grand Unification*, ed. J. Arafune, 118 (1987), Singapore, World Scientific.

[47] Y. Totsuka, In *Proc. Int. Symposium on Underground Physics Experiments*, ed. K. Nakamura, 129 (1990), Univ. of Tokyo.

[48] M. Takita, In *Frontiers of Neutrino Astrophysics*, ed. Y. Suzuki and K. Nakamura, 135 (1993). Tokyo:Universal Academic Press.

[49] R.S. Raghavan, 1991. In *Proc. 25th Int. Conf. High Energy Physics*, ed. K.K Phua and Y. Yamaguchi, 482 (1991). Japan : South Asia Theor. Phys. Assoc. and Phys. Soc.

[50] M. Campanella, In *Proc. 3rd Int. Workshop on Neutrino Telescopes*, ed. M Baldo-Ceolin, (1992) p. 73. Venice: Univ. di Padova

[51] K. Lande, To appear in the *Proc. 22nd Int. Conf. on Cosmic Ray Physics* (1993).

[52] W.C. Haxton, *Phys. Rev. Lett.* 60 (1988) 768-71.

[53] C. Rubia, *INFN Publication* (1985) INFN/AE-85-7.

[54] S.R. Bandler, *Phys. Rev. Lett.* 68 (1992) 2429-32; J.S. Adams et. al., *Phys. Lett. B*. 341 (1995) 431.

[55] G. Laurenti, S. Tzamarias, G. Bonvicini, P. Krastev, A. Zichichi, et. al., (1994). INFN preprint.

12